TRAPPII regulates exocytic Golgi exit by mediating nucleotide exchange on the Ypt31 ortholog RabE^{RAB11}

Mario Pinar[a], Herbert N. Arst Jr.[a,b], Areti Pantazopoulou[a], Víctor G. Tagua[a], Vivian de los Ríos[a], Javier Rodríguez-Salarichs[c], J. Fernando Díaz[c], and Miguel A. Peñalva[a,1]

Departments of [a]Cellular and Molecular Biology, and [c]Chemical and Physical Biology, Centro de Investigaciones Biológicas, Consejo Superior de Investigaciones Científicas, 28040 Madrid, Spain; and [b]Section of Microbiology, Imperial College London, London SW7 2AZ, United Kingdom

The oligomeric complex transport protein particle I (TRAPPI) mediates nucleotide exchange on the RAB GTPase RAB1/Ypt1. TRAPPII is composed of TRAPPI plus three additional subunits, Trs120, Trs130, and Trs65. Unclear is whether TRAPPII mediates nucleotide exchange on RAB1/Ypt1, RAB11/Ypt31, or both. In *Aspergillus nidulans*, RabO^{RAB1} resides in the Golgi, RabE^{RAB11} localizes to exocytic post-Golgi carriers undergoing transport to the apex, and *hypA* encodes Trs120. RabE^{RAB11}, but not RabO^{RAB1}, immunoprecipitates contain Trs120/Trs130/Trs65, demonstrating specific association of TRAPPII with RabE^{RAB11} in vivo. *hypA1^{ts}* rapidly shifts RabE^{RAB11}, but not RabO^{RAB1}, to the cytosol, consistent with HypA^{Trs120} being specifically required for RabE^{RAB11} activation. Missense mutations rescuing *hypA1^{ts}* at 42 °C mapped to *rabE*, affecting seven residues. Substitutions in six, of which four resulted in 7- to 36-fold accelerated GDP release, rescued lethality associated to TRAPPII deficiency, whereas equivalent substitutions in RabO^{RAB1} did not, establishing that the essential role of TRAPPII is facilitating RabE^{RAB11} nucleotide exchange. In vitro, TRAPPII purified with HypA^{Trs120}-S-tag accelerates nucleotide exchange on RabE^{RAB11} and, paradoxically, to a lesser yet substantial extent, on RabO^{RAB1}. Evidence obtained by exploiting *hypA1*-mediated destabilization of HypA^{Trs120}/HypC^{Trs130}/Trs65 assembly onto the TRAPPI core indicates that these subunits sculpt a second RAB binding site on TRAPP apparently independent from that for RabO^{RAB1}, which would explain TRAPPII in vitro activity on two RABs. Using *A. nidulans* in vivo microscopy, we show that HypA^{Trs120} colocalizes with RabE^{RAB11}, arriving at late Golgi cisternae as they dissipate into exocytic carriers. Thus, TRAPPII marks, and possibly determines, the Golgi–to–post-Golgi transition.

Golgi | post-Golgi carriers | GTPase | GEF | *Aspergillus*

A conceptual advance in understanding traffic across the Golgi came from the visualization of fungal cisternae as a set of membranous compartments forming by coalescence of endoplasmic reticulum-derived COPII traffic and undergoing changes in composition until they dissipate into carriers destined to the plasma membrane or endosomes (1–5).

RAB GTPases [and, by extension, their GTPase-activating (GAP) and guanine nucleotide exchange factor (GEF) regulators] are major determinants of protein and lipid composition of membranous compartments (6). In fungi, anterograde Golgi traffic is governed by RAB1 and RAB11 homologs. In *Saccharomyces cerevisiae* and *Aspergillus nidulans*, RAB1 homologs (Ypt1 and RabO, respectively) (7, 8) mediate biogenesis of Golgi cisternae and anterograde traffic across them, whereas RAB11 homologs (Ypt31/Ypt32 and RabE, respectively) (9, 10) mediate Golgi exit of exocytic carriers and control their trafficking to the plasma membrane. The sharp functional boundary between Ypt1 and Ypt31/Ypt32 is determined, at least in part, by an anticurrent cascade in which Gyp1, the GAP for Ypt1, is an effector of Ypt31/Ypt32, thus ensuring minimal overlap of the GTPases on the same membranes (11). In *A. nidulans* hyphae, late Golgi cisternae (LGCs) are separated from the apex (the target of

exocytic carriers) by a few microns gap (12). When RabE is recruited to LGCs, these lose Golgi identity, engage motors, and break up into post-Golgi carriers that are delivered to the apex, where they accumulate before fusing with the plasma membrane (9). In contrast with RabE predominating in these carriers, RabO preferentially localizes to the Golgi (8), illustrating the sharp boundary between their respective functional domains.

The countercurrent Golgi RAB GAP cascade would act in concert with a RAB cascade by which early Ypt1 membranes mature into late Ypt31/Ypt32 membranes. This maturation would involve conversion between two different versions of a multimeric GEF, denoted TRAPPI and TRAPPII (13). [A third version, TRAPPIII, specifically regulates the Ypt1 role in autophagy (14).] TRAPPI mediates Ypt1 activation at the early Golgi; TRAPPII is composed of TRAPPI plus additional subunits, Trs65, Trs120, and Trs130, putatively shifting TRAPP GEF specificity from Ypt1 toward late Golgi-acting Ypt31/Ypt32 (13). However, another report challenged this interpretation by finding that in vitro TRAPPII mediates nucleotide exchange on Ypt1, but not on Ypt31/Ypt32, efficiently (15), leading others to conclude that both TRAPPI and TRAPPII target Ypt1, but the latter mediates Ypt1 activation specifically in the late Golgi (16), thus leaving open the identity of the fungal RAB11 GEF.

hypA encodes *A. nidulans* Trs120 (17). The conditional *hypA1^{ts}* mutation prevents growth at the restrictive temperature, consistent with *hypA* playing an essential role in exocytosis. We selected extragenic mutations bypassing this role. Remarkably,

Significance

Ypt1 and Ypt31/32 RAB GTPases regulate traffic across the Golgi. Both are activated by TRAPP, an oligomeric GEF. Three TRAPP versions share the same core subunits. TRAPPI and TRAPPIII activate Ypt1. The third, TRAPPII, composed of TRAPPI plus specific subunits, appears to act specifically on Ypt31, but this role has been disputed. By combining the resolving power of fungal genetics with biochemical assays, we establish that the physiological target of TRAPPII is RabE, the *Aspergillus* Ypt31 ortholog. However, our data suggest that TRAPPII contains independent binding sites for RabE and RabO (Ypt1), possibly explaining its relative lack of discrimination in vitro. TRAPPII arrives at Golgi cisternae preceding their dissipation into carriers, determining the Golgi–to–post-Golgi transition through RabE recruitment.

with a single exception, these mutations mapped to *rabE*. Genetic and biochemical analysis of these mutations and nucleotide exchange assays using affinity-purified TRAPPII established that TRAPPII serves, in vivo and in vitro, as GEF for RabE.

Results

HypA^Trs120 Is a Component of TRAPPII That, Like Other TRAPPII-Specific Components, Associates with RabE in Vivo.

In agreement with their predicted role in exocytosis, HypA^Trs120 and HypC^Trs130 are essential (Fig. S1 *A and B*), with *hypAΔ* and *hypCΔ* conidia arresting polar growth with typical "hypercellular" (*hyp*) morphology (17) shortly after germination (Fig. S1 *A and B*). Also essential is nucleotide exchange-mediating TRAPP "core" subunit BetT^Bet3 (Fig. S1*C*) (15), as are its predicted substrates, RabO and RabE (8, 9). We used HypA^Trs120, endogenously tagged with S-peptide (18), to purify associated proteins. HypA^Trs120 pulled down TRAPPII from extracts, as judged from copurification of the two other TRAPPII-specific subunits, Trs65 and Trs130, and of all six TRAPP core subunits (Fig. 1*A* and Table S1). To investigate RAB association with TRAPPII, we raised antisera against RabE and RabO (Fig. 1*B*) and used them in immunoprecipitation experiments, with anti-SarA^SAR1 antiserum (19) as control. TRAPPII-specific subunits HypA^Trs120, HypC^Trs130, and Trs65 copurified with RabE but not with RabO or SarA^SAR1, whereas, as predicted (14), TRAPPIII-specific subunit Trs85 copurified solely with RabO (Fig. 1*C*). Thus, in vivo TRAPPII associates preferentially with RabE.
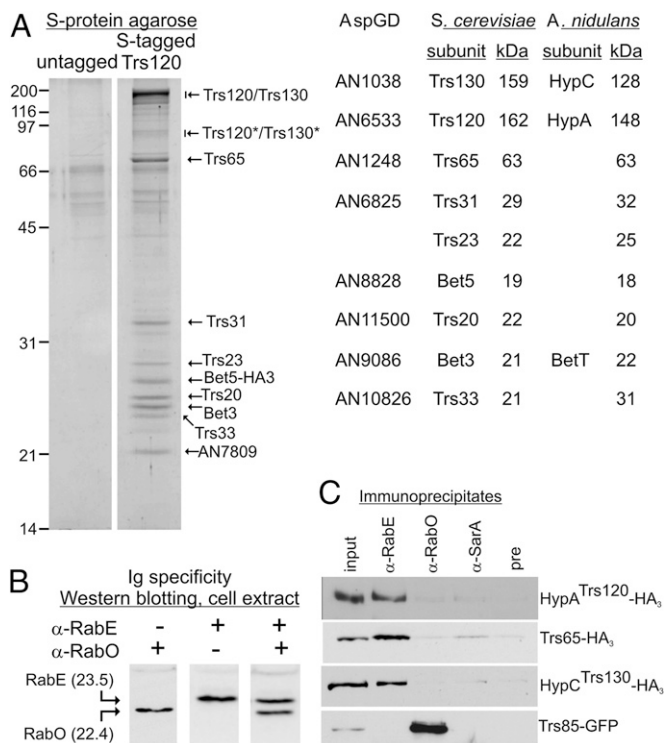

Fig. 1. Proteins associating with HypA^Trs120. (*A*) SDS/PAGE analysis of affinity column-bound material showing that S-tagged HypA^Trs120 pulls down TRAPPII from cell extracts. The identity of the different bands was determined by mass spectrometry (Table S1) (asterisks, proteolysis products). Sizes, kilodaltons. (*B*) Specificity controls for RabE and RabO rabbit antisera. Alkaline lysates were analyzed by Western blotting with the indicated antisera. The two RABs differ in ~1 kDa (in brackets). (*C*) Western blotting of epitope-tagged TRAPP components in immunoprecipitates of cell extracts with indicated antisera (pre, preimmune). SarA is *A. nidulans* Sar1.
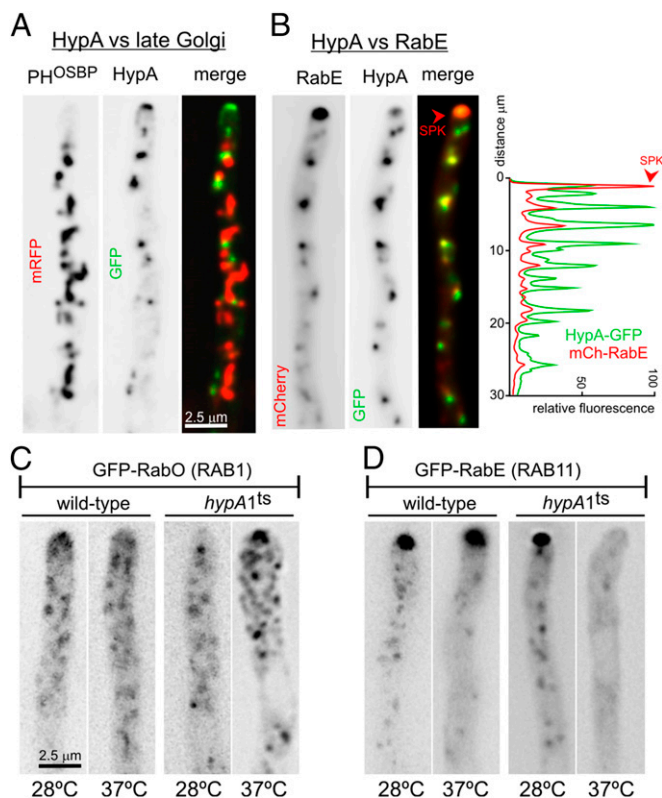

Fig. 2. Subcellular studies. (*A*) Localization of endogenously tagged HypA-GFP compared with LGC labeled with PH^OSBP. (*B*) HypA-GFP colocalizes with RabE. Plot shows colocalization and relative signal intensities of individual channels. (*C*) In *hypA1^ts* hyphae, GFP-RabO localizes to Golgi puncta both at 28 °C and after 50-min incubation at 37 °C. (*D*) GFP-RabE is rapidly and completely displaced from post-Golgi membranes to the cytosol upon shifting *hypA1* cells from 28 to 37 °C.

HypA^Trs120 Colocalizes with RabE in Post-Golgi Membranes.

RabE is a marker of post-Golgi exocytic carriers that arise from LGC and are transported over microns to the apex, where they accumulate, forming the Spitzenkörper (SPK) (9). Endogenously GFP-tagged HypA^Trs120 localizes to puncta that do not colocalize with SedV^Sed5 early Golgi (Fig. S2*A*) and barely colocalize with late Golgi PH^OSBP cisternae (Fig. 2*A* and Movie S1). Golgi-disturbing drug brefeldin A (BFA) leads to coalescence of Golgi residents (including RabO) into conspicuous aggregates (8, 12, 20). In sharp contrast, BFA delocalizes post-Golgi RabE to a haze (9), and HypA^Trs120 behaved like RabE (Fig. S2*B*). Thus, although HypA^Trs120 recruitment to puncta requires a functional Golgi, HypA^Trs120 itself localizes near or beyond Golgi boundaries.

Kymographs derived from time-resolved images showed that HypA^Trs120 arrives at LGC at the latest stages of their ~2-min life cycle, being recruited as they dissipate (Fig. S2*C*) and, like RabE (9), staying only transiently at these positions. Indeed, HypA^Trs120 colocalizes with RabE (Fig. 2*B*; 94% of *n* = 89 HypA^Trs120-GFP puncta colocalize with mCh-RabE and 99% of *n* = 85 mCh-RabE puncta contain HypA^Trs120-GFP; 12 hyphae). Kymographs further established that HypA^Trs120 and RabE signals colocalized across time (Fig. S2*D*). Notably, compared with RabE, which largely accumulates in the SPK, HypA^Trs120 is "displaced" toward maternal cisternae, with more conspicuous labeling of Golgi-associated puncta and lesser accumulation at the SPK (Fig. 2*B*). Thus, HypA^Trs120 localization is consistent with arrival at LGC preceding RabE recruitment, as expected for a RabE GEF.

CELL BIOLOGY

HypA^Trs120 Is Required for Localization of RabE to Membranes. At 37 °C, *hypA1^ts* prevents growth almost completely (17, 21). Temperature shift from 28 to 37 °C results in abnormal swelling of *hypA1^ts* cell tips, correlating with mislocalization of the secretory v-SNARE SynA from the apical crescent (20, 22) to internal structures (Fig. S2E). Thus, HypA^Trs120 inactivation arrests exocytosis. Although GDP-locking mutations delocalize RabO and RabE to the cytosol (8, 9), *hypA1* did not prevent GFP-RabO localization to Golgi puncta (Fig. 2C), as reported for *S. cerevisiae trs130^ts* and GFP-Ypt1 (13). In sharp contrast, *hypA1* delocalized RabE to the cytosol within 20 min at 37 °C (Fig. 2D). Thus, HypA^Trs120 mediates RabE, but not RabO, recruitment to membranes.

rabE Mutations Bypass TRAPPII. Compelling evidence that TRAPPII is the RabE GEF came from mutations rescuing viability of *hypA1^ts* cells at 42 °C. We isolated 25 single extragenic suppressor mutations (segregating 1:2:1 in backcrosses). By classical genetics, we mapped one, *su22hypA1*, to a ∼380-kb chromosome VIII region that, notably, includes *rabE* (Scheme S1). Sequencing showed that *su22hypA1* is a missense N122H mutation in *rabE* involving Asn122 in the nucleotide-binding pocket (Table 1), strongly suggesting that N122H effects *hypA1^ts* suppression. Twenty-three of the remaining 24 strains have single missense mutations in *rabE* (Table 1), with certain RabE residues recurrently affected, suggesting that these are mechanistically important for suppression. To establish that these mutations effect suppression, we chose F29S, D37G, M118V, N122H, K123R, D125E, and G185K *rabE* substitutions (one for each affected codon) and PCR-amplified *rabE* fragments containing the respective mutations, with which we reconstructed, in a *hypA1^ts* background, the mutant alleles by transformation. "Engineered" and "classical" strains were indistinguishable in their degree of *hypA1^ts* suppression (Fig. 3A).

The above findings, and the fact that nearly all *hypA1^ts* suppressors lie in *rabE*, strongly indicate that HypA^Trs120 is a component of a RabE GEF. However, it was formally possible that *rabO* mutations might also be capable of suppressing *hypA1* but were not recovered. To address this possibility, we constructed two gene-replaced *rabO* alleles encoding mutant K122R and D124E RabO, equivalent to mutant K123R and D125E RabE, respectively (the choice of these mutations will become evident below). We demonstrated that, although mutant proteins are stably expressed (Fig. 3B), neither *rabO* mutation suppresses *hypA1^ts* (Fig. 3C). Indeed, genetic mapping showed that the only extragenic suppressor not in *rabE* is also not in *rabO*. We next tested whether RabE F29S, D37G, M118V, N122H, K123R, D125E, and G185K bypass the complete absence of TRAPPII subunits Trs120 and Trs130 by deleting *hypA* or *hypC* in the mutant *rabE* backgrounds. In every case except M118V, *rabE* mutations substantially rescued viability of *hypAΔ* and *hypCΔ* (Fig. 3D; M118V rescued very weakly). In sharp contrast, double mutants with *betTΔ* were essentially unviable (Fig. S3) (F29S,

N122H, K123R, and D125E permitted residual growth; see below). As expected, *rabE^D125E* did not rescue *rabOΔ* (Fig. 3D). Therefore, genetic data support the contention that RabE substitutions bypass the role of TRAPPII as GEF, but not the role of the TRAPP core: BetT^Bet3 remains essential because, unlike HypA^Trs120 and HypC^Trs130, it is directly involved in mediating nucleotide exchange on both RabO and RabE (13–15).

F29S, N122H, K123R, and D125E Accelerate Intrinsic GDP Release. RabE Asn122, Lys123, and Asp125 lie within a NKxD motif contributing to the guanine nucleotide binding site in virtually all Ras superfamily proteins (Fig. 4A) (23, 24) including RAS itself, in which NKxD substitutions are oncogenic (25, 26). In yeast Ypt7, substitutions of Lys or Asp residues bypass the GEF component Ccz1 (27), having been proposed to enhance intrinsic dissociation rates by debilitating the interaction with the guanine nucleotide (28, 29). Thus, we hypothesized that some RabE substitutions would similarly bypass TRAPPII and proceeded to characterize the kinetics of purified WT and mutant RabE proteins (Fig. 4A and Fig. S4). Lys123Arg and Asp125Glu accelerated nucleotide release by 35-fold at 25 °C, whereas Asn122His showed a sixfold to eightfold increase (Fig. 4A). These data provided strong support for the above interpretation and, importantly, established that increasing the spontaneous RabE GDP release rate (formally equivalent to gain of function) suffices to bypass the roles of HypA^Trs120 and HypC^Trs130, strongly implicating HypA^Trs120, and by extension TRAPPII, in mediating nucleotide exchange on RabE. This conclusion was buttressed by the finding that F29S, the fourth member of the "stronger suppressor" class, accelerated GDP release >25-fold at 25 °C. As modeled with hsRAB11b (30), Phe29 is located at α-helix 1, whose N terminus contributes the "P-loop Lys" (Lys22 in RabE) involved in GDP release in Ras superfamily members (31, 32) (Fig. 4B). Indeed, in Ypt1, a glutamate contributed by TRAPP Bet3 mediates removal of this Lys side chain from its interaction with nucleotide phosphates (15, 32). Phe29 makes a stacking interaction with conserved Phe163 (Fig. 4B), which would be disrupted if the Phe29 aromatic ring were missing, likely shifting α-helix 1 and Lys22 in a way that destabilizes the nucleotide. Phe29Cys and Phe29Ser substitutions accounted for ∼40% of the *hypA1* suppressors (Table 1).

The remaining substitutions bypass TRAPPII without increasing (Gly185Lys), or increasing modestly (Asp37Gly, Met118Val), nucleotide release (Fig. 4A). We discarded the possibility that they shift RabE toward the GTP conformation by exploiting, in GST pull-down assays, the strong preference that GDP dissociation inhibitor (GDI) has for GDP Rabs (Fig. 4C). RabE-GDP, but not RabE-GTP, efficiently pulled (HA)3-tagged GdiA (GDI) from cell extracts. Consistent with their reduced affinity for GDP, F29S, N122H, K123R, and D125E mutants were incapable of pulling down GDI when loaded with 0.1 mM GDP, but became competent if GDP was raised to 10 mM (Fig. 4C), further validating the assay. In these assays, D37G, M118V, and G185K behaved as WT (Fig. 4C), ruling out the possibility that these substitutions promote the active conformation, or prevent interaction with GDI. Asp37 is located in switch I (Fig. S5), in a position that does not contact GAPs in available RAB-GAP structures (33–35). Met118 is involved in a conserved-with-RAB11b hydrophobic network that "stitches" the C-terminal α-helix 5 with the central platform of β-strands (Fig. S6). Of note, Rab3A α-helix 5 residues contribute to one of the RAB specificity-determining motifs (36) and are involved in binding to its effector rabphilin (37). Gly185Lys substitution in the C-terminal hypervariable region is remarkable. The structure of this region is only available for Ypt1 complexed with GDI, which "chaperones" this otherwise unstructured extension (38). However, Gly185Lys does not prevent GDI binding (Fig. 4C) nor does it increase GDP release

Table 1. Suppressors of hypA1

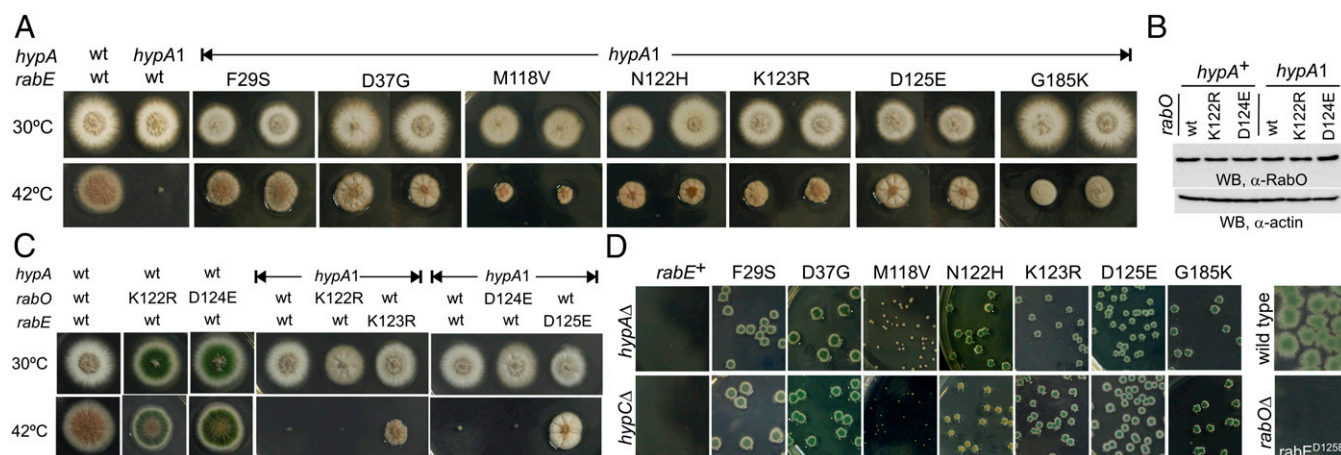| *rabE* alleles	Codon change	cDNA change	aa change
3, 5, 20, 23	TTT > TCT	T86C	F29S
4, 13, 16, 17, 21, 26	TTT > TGT	T86G	F29C
1, 8, 14, 29	GAT > GGT	A110G	D37G
12, 24, 27	GAT > GCT	A110C	D37A
31	ATG > GTG	A352G	M118V
9, 22, 30	AAT > CAT	A364C	N122H
25	AAG > AGG	A368G	K123R
32	AAG > CAG	A367C	K123Q
28	GAT > GAA	T375A	D125E
11	GGA > AAA	G553A G554A	G185K

Fig. 3. Growth phenotypes of *hypA* suppressors. (*A*) Growth phenotypes: "classical" *hypA1 rabE* suppressor double-mutant strains (*Left*) alongside engineered strains carrying equivalent *rabE* alleles reconstituted in a *hypA1* background (*Right*). (*B*) Western blot showing that RabO K122R and D124E substitutions do not affect RabO levels. (*C*) RabO K122R or D124E do not suppress *hypA1*. (*D*) Rescue of *hypAΔ* and *hypCΔ* lethality by *rabE* mutations: *hypA*, *hypC*, or *rabO* were deleted in the indicated *rabE* mutant backgrounds. Conidiospore suspensions were plated to give isolated colonies if viable. For combinations leading to lethal or severely debilitating phenotypes, conidiospores were obtained from heterokaryons.

(Fig. 4*A*), which raises the intriguing possibility that the hypervariable domain contributes to the active RAB conformation.

Nucleotide Exchange Assays with TRAPPII. We demonstrated that TRAPPII is a RabE GEF using complex purified from WT cell extracts with S-tagged HypA^Trs120 (Fig. 1*A* and Fig. S7). We confirmed, by anti-HA Western blotting, that this fraction contained HypC^Trs130 and Trs65 (Fig. 5*A*), and used it for in vitro assays with purified RabE, RabO, and RabB^RAB5, loaded with mant-GDP, to determine the basal and TRAPPII-stimulated release of the probe from the RABs in presence of excess GTP. TRAPPII did not stimulate nucleotide exchange on RabB^RAB5

(Fig. S8), indicating specificity. In contrast, TRAPPII stimulated 2.4-fold nucleotide exchange on RabO. Notably, stimulation was even higher for RabE (3.3-fold), although RabE had faster "basal" nucleotide exchange than RabO (Fig. 5 *B* and *C* and Fig. S8). To implicate directly HypA^Trs120 in GEF activity on RabE, we attempted to pull out mutant *hypA1* TRAPPII from 28 °C cells endogenously expressing HypA1-S-tag or WT Trs65-S-tag baits. However, TRAPP yields were negligible (Fig. S7), indicating that *hypA1* destabilizes TRAPPII [Trs120 has a central role in TRAPPII assembly (39)].

Next, we purified WT and *hypA1* TRAPP with S-tagged Trs33, a component of TRAPPI and TRAPPII (14) interacting with Trs120
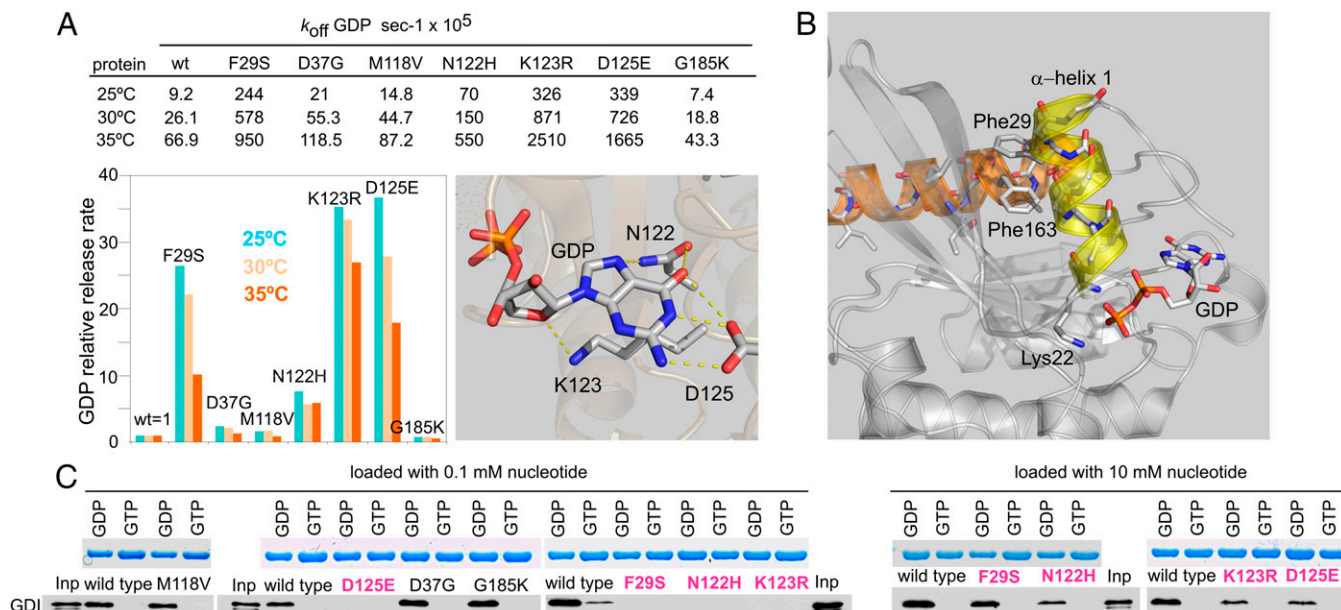

Fig. 4. Biochemical characterization of mutant RabE proteins. (*A*) GDP dissociation constants of RabE mutants. The bar diagram depicts these figures relative to the WT. The drawing shows polar contacts (dotted lines) of N122, K123, and D125 with guanosine in the RAB11b structure. (*B*) Phe29 is located in α-helix 1–containing Lys22 at its N terminus. Lys22 side chain projects into the nucleotide pocket. Figure prepared with PyMol, using Protein Data Bank entry 2F9L (30). RabE residues 4–179 differ from RAB11b in only 15 positions. (*C*) GST pull downs of GdiA-HA3 from cell extracts. Input (Inp), 2% of pulled-down material. Coomassie staining shows GST-RabE fusion proteins in the pulled-down material. Pulled-down GdiA (GDI) was detected by anti-HA Western blotting. Red font is used for mutants having accelerated GDP release.
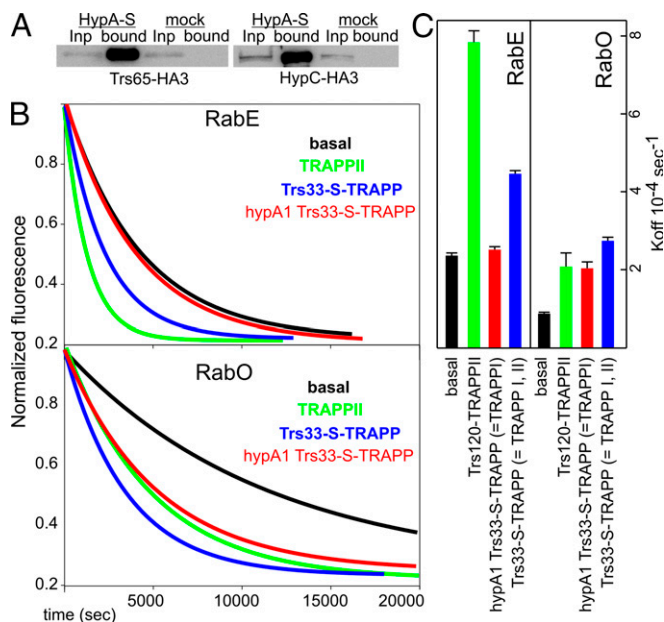
Fig. 5. TRAPPII-stimulated nucleotide exchange. (*A*) Western blots showing that TRAPP purified with S-tagged HypA^{Trs120} contains HpC^{Trs130} and Trs65. Inp, input (1% of material); mock, pull down with untagged HypA^{Trs120}. (*B*) TRAPP-mediated stimulation of basal nucleotide exchange rates. Five micromolar GST-RABs, preloaded with mant-GDP, were incubated in the presence of 50 μM GTP with or without indicated TRAPP fractions (Fig. S7). The reactions were followed by the decrease in the 437-nm FRET fluorescence emission of RAB-bound mant-GDP. Curves are the average of triplicate experiments (Fig. S8). (*C*) Data were adjusted to exponential curves to obtain observed rate constants for basal and TRAPP-stimulated mant-GDP dissociation.

and Bet3 (40, 41). Trs33-S-tag TRAPP, like HypA^{Trs120}-S-tag TRAPP, contained TRAPPII-specific subunits when purified from WT cells (Fig. S7) and, consistently, stimulated both RabO and RabE (Fig. 5 *B* and *C* and Fig. S8). In sharp contrast, TRAPP purified with Trs33-S-tag from *hypA1* cells contained TRAPPI subunits, but lacked Trs130, Trs120, and Trs65 (Fig. S7). This TRAPPI had the same activity on RabO as HypA^{Trs120}-S TRAPPII and Trs33-S TRAPP from the WT but had no effect on RabE (Fig. 5 *B* and *C* and Fig. S8). Therefore, the loss of Trs120 and other TRAPPII subunits from TRAPP implies the loss of GEF activity specifically on RabE, showing that Trs120 contributes to a RabE binding site in TRAPPII. Moreover, the fact that TRAPPII and TRAPPI have essentially the same activity on RabO shows that Trs120/Trs130/Trs65 sculpt a RabE binding site in TRAPPII without occluding that for RabO, which suggests that TRAPPII contains independent binding sites for these RABs.

Discussion

In *A. nidulans*, RabE resides in post-Golgi carriers arising from LGC by maturation (9) and *hypA* encodes TRAPPII Trs120. Of seven RabE mutants rescuing *hypA1* mutants at 42 °C, six bypassed the lethal ablation of HypA^{Trs120} or HypC^{Trs130}, including F29S, N122H, K123R, and D125E, resulting in accelerated GDP release. In contrast, K122R and D124E mutants of RabO were unable to rescue *hypA1*. RabE "GDP release" mutations rescued BetT^{Bet3} ablation only marginally, indicating that they cannot bypass a complete core TRAPP deficiency simultaneously affecting RabE and RabO. Hence TRAPPII acts upstream of nucleotide exchange for a RAB11, but not for a RAB1, ortholog. Given that TRAPPII-specific subunits coimmunoprecipitate with RabE, but not with RabO, that *hypA1* affecting Trs120 shifts RabE, but not RabO, to the cytosol, that

TRAPPII, when affinity-purified with S-tagged Trs120, stimulates GDP/GTP exchange on RabE to a greater extent than on RabO, and, importantly, that HypA^{Trs120} colocalizes with RabE in post-Golgi domains, we conclude that in vivo TRAPPII acts specifically as RabE GEF, concurring with Morozova et al. (13).

Genetic evidence that TRAPPII components act upstream of a RAB11 exists also for *S. cerevisiae*: increased *YPT31/32* dosage vigorously rescues lethality of *trs130Δ* (42) and *trs130*^{ts} (43) and, weakly, that of *trs120Δ* strains (42), but does not bypass core TRAPP mutants, nor does increased *YPT1* dosage bypass *trs130Δ* (42). By exploiting a negative genetic interaction between *YPT31* and *PIK1* (encoding PtsIns 4-kinase), others located the physiological role of Ypt31 to the late Golgi, and showed that TRAPPII-specific subunits act upstream of Ypt31 (44).

What explains TRAPPII GEF activity on RabO? Although elution of TRAPPII from affinity beads may partially dissociate the complex, yielding some TRAPPI, our data indicate instead that TRAPPII dual activity in vitro results from its containing independent binding sites for RabE and RabO: TRAPPII, stripped from Trs120, Trs130, and Trs65 with the destabilizing mutation *hypA1* (i.e., TRAPPI), has the same activity on RabO as TRAPPII, but none on RabE. TRAPPI binding to Ypt1 is mediated by a dimer of longin domains (LDs) contributed by Trs23/Bet5 (15). Indeed, LDs form platforms binding small GTPases (45). Thus, Levine et al. (45) proposed that LDs such as those present in TRAPP Tca17 or Trs20 interact with LD-related folds specifically contributed by TRAPPII subunits to sculpt a second binding site for RAB11 orthologs. Suggestively, Trs120 (HypA) is incorporated into TRAPPII through direct interaction with LD-containing Trs20 (39, 46). The presence of independent binding sites for the two RABs in the context of a common GEF mechanism would explain conflicting in vitro experiments on the nature of the yeast TRAPPII substrate(s). We speculate that in vivo the likely existence of independent binding sites for RabE and RabO in TRAPPII might facilitate the reported cross talk between Ypt1, Ypt31, and Sec7 that directs traffic in LGC (47).

Ypt31 was reported to localize to Sec7-containing LGC (44). Exquisite time and spatial resolution achievable for in vivo microscopy of *A. nidulans* permitted us to demonstrate that RabE resides in post-Golgi carriers that arise by maturation of LGC and subsequently travel to the apical SPK (9). For any given LGC, transition of Golgi to post-Golgi identity is landmarked by the diminution of Sec7 and PH^{OSBP} probe (codetecting Arf1-PtdIns4P) content that takes place as RabE is recruited (9). HypA^{Trs120} strictly colocalizes across time with RabE in maternal LGC locations, but its signal markedly decreases as carriers travel to the SPK, consistent with HypA^{Trs120} acting upstream of RabE, at the transition from LG to post-Golgi identity. Thus, Sec7 is a compositional feature of the carrier formation stage (late Golgi/trans-Golgi network) of Golgi cisternae (4), whereas TRAPPII would be the earliest marker of post-Golgi commitment in the chain of maturation events ultimately leading to RabE acquisition.

Materials and Methods

A. nidulans Strains, Genetic Manipulation, in Vivo Microscopy, and Protein Tagging. Standard media, growth conditions, and genetic methodology were used (9, 48, 49). Strains are in Table S2. Heterokaryon rescue for assessment of lethality was as described (50). Epifluorescence microscopy of actively growing cells was carried out with a Leica DMI6000 microscope (9), using reported fluorescent markers and conditions for temperature shift-up experiments "on the stage" (8, 9, 21). *hypA*, *hypA1*, *hypC*, *trs65*, *trs33*, *bet5*, *trs85*, and *gdiA* were C-terminally tagged by gene replacement (with GFP, HA3, or S-tag as required), such that tagged proteins were expressed at physiological levels and represented the only source of protein.

Biochemical Assays. RabE, RabO, and RabB^{RAB5} were expressed in *Escherichia coli* fused to GST and purified on glutathione-Sepharose 4B (51). GDP release rates of WT and mutant GDP-loaded RabE were determined by monitoring

the fluorescence increase resulting from exchanging GDP in the nucleotide binding pocket by mant-GDP, present in excess in the reaction (*SI Materials and Methods*) (52). Interaction of RabE with nucleotides is defined by the following equilibria:

$$GDP::RAB \underset{k_{+1}}{\overset{k_{-1}}{\rightleftharpoons}} GDP, \, mantGDP, \, RAB \underset{k_{-2}}{\overset{k_{+2}}{\rightleftharpoons}} mantGDP::RAB.$$

Presence of an excess of mant-GDP over GDP results in pseudo–first-order conditions under which $k{+}2{\bullet}[RabE]{\bullet}[mant{-}GDP] \gg k{+}1{\bullet}[RabE]{\bullet}[GDP]$. Thus, $d[mant{-}GDP::RabE]/dt = k{-}1{\bullet}[GDP::RabE]$, and the increase in fluorescence reflecting the decay in [GDP::RabE] can be fitted to the exponential curve $F = Fo + a(1 - e^{(-k-1{\bullet}t)})$, from which we derived k_{-1} (Fig. S5) (*a* is the total fluorescence increase to plateau, *F* is fluorescence, and *t* is time).

TRAPP preparations were obtained by S-tag one-step affinity purification as described (53) (*SI Materials and Methods*). GEF assays measured TRAPP-stimulated release of mant-GDP by GST-RABs at 30 °C, in the presence of excess GTP. Five micromolar mant-GDP GST-RAB was incubated with 50 µM GTP and S-tagged (HypA[Trs120] or Trs33) TRAPP. The reaction was followed by the decrease in fluorescence at 437 nm, and the resulting exponential curve was used to obtain observed dissociation rate constants for mant-GDP in the presence of TRAPP preparations (*SI Materials and Methods*). TRAPPII obtained from WT HypA[Trs120]-S tag cell extract contained ~2 µM complex, estimated by comparison of the Trs33 band with a standard. Mock extract consisted of S-tag column eluate obtained from untagged cell extract. HypA1-S-tag (expressed from a gene-replaced, S-tagged *hypA*1 allele) TRAPP fraction, or mutant Trs33-S-tag fraction was obtained from cells cultured at 30 °C. S-agarose affinity eluates corresponded to 300 mg of starting WT or *hypA*1 protein extract.

1. Wooding S, Pelham HRB (1998) The dynamics of Golgi protein traffic visualized in living yeast cells. *Mol Biol Cell* 9(9):2667–2680.
2. Glick BS, Nakano A (2009) Membrane traffic within the Golgi apparatus. *Annu Rev Cell Dev Biol* 25:113–132.
3. Losev E, et al. (2006) Golgi maturation visualized in living yeast. *Nature* 441(7096):1002–1006.
4. Day KJ, Staehelin LA, Glick BS (2013) A three-stage model of Golgi structure and function. *Histochem Cell Biol* 140(3):239–249.
5. Matsuura-Tokita K, Takeuchi M, Ichihara A, Mikuriya K, Nakano A (2006) Live imaging of yeast Golgi cisternal maturation. *Nature* 441(7096):1007–1010.
6. Behnia R, Munro S (2005) Organelle identity and the signposts for membrane traffic. *Nature* 438(7068):597–604.
7. Jedd G, Richardson C, Litt R, Segev N (1995) The Ypt1 GTPase is essential for the first two steps of the yeast secretory pathway. *J Cell Biol* 131(3):583–590.
8. Pinar M, Pantazopoulou A, Arst HN, Jr, Peñalva MA (2013) Acute inactivation of the *Aspergillus nidulans* Golgi membrane fusion machinery: Correlation of apical extension arrest and tip swelling with cisternal disorganization. *Mol Microbiol* 89(2):228–248.
9. Pantazopoulou A, Pinar M, Xiang X, Peñalva MA (2014) Maturation of late Golgi cisternae into RabE[RAB11] exocytic post-Golgi carriers visualized *in vivo*. *Mol Biol Cell* 25(16):2428–2443.
10. Jedd G, Mulholland J, Segev N (1997) Two new Ypt GTPases are required for exit from the yeast trans-Golgi compartment. *J Cell Biol* 137(3):563–580.
11. Rivera-Molina FE, Novick PJ (2009) A Rab GAP cascade defines the boundary between two Rab GTPases on the secretory pathway. *Proc Natl Acad Sci USA* 106(34):14408–14413.
12. Pantazopoulou A, Peñalva MA (2009) Organization and dynamics of the *Aspergillus nidulans* Golgi during apical extension and mitosis. *Mol Biol Cell* 20(20):4335–4347.
13. Morozova N, et al. (2006) TRAPPII subunits are required for the specificity switch of a Ypt-Rab GEF. *Nat Cell Biol* 8(11):1263–1269.
14. Lynch-Day MA, et al. (2010) Trs85 directs a Ypt1 GEF, TRAPPIII, to the phagophore to promote autophagy. *Proc Natl Acad Sci USA* 107(17):7811–7816.
15. Cai Y, et al. (2008) The structural basis for activation of the Rab Ypt1p by the TRAPP membrane-tethering complexes. *Cell* 133(7):1202–1213.
16. Barrowman J, Bhandari D, Reinisch K, Ferro-Novick S (2010) TRAPP complexes in membrane traffic: Convergence through a common Rab. *Nat Rev Mol Cell Biol* 11(11):759–763.
17. Shi X, Sha Y, Kaminskyj S (2004) Aspergillus nidulans *hypA* regulates morphogenesis through the secretion pathway. *Fungal Genet Biol* 41(1):75–88.
18. De Souza CP, Hashmi SB, Osmani AH, Osmani SA (2014) Application of a new dual localization-affinity purification tag reveals novel aspects of protein kinase biology in *Aspergillus nidulans*. *PLoS One* 9(3):e90911.
19. Hernández-González M, Peñalva MA, Pantazopoulou A (2015) Conditional inactivation of *Aspergillus nidulans* sarA(SAR1) uncovers the morphogenetic potential of regulating endoplasmic reticulum (ER) exit. *Mol Microbiol* 95(3):491–508.
20. Pantazopoulou A, Peñalva MA (2011) Characterization of *Aspergillus nidulans* RabC/Rab6. *Traffic* 12(4):386–406.
21. Pinar M, Pantazopoulou A, Peñalva MA (2013) Live-cell imaging of *Aspergillus nidulans* autophagy: RAB1 dependence, Golgi independence and ER involvement. *Autophagy* 9(7):1024–1043.
22. Taheri-Talesh N, et al. (2008) The tip growth apparatus of *Aspergillus nidulans*. *Mol Biol Cell* 19(4):1439–1449.
23. Dever TE, Glynias MJ, Merrick WC (1987) GTP-binding domain: Three consensus sequence elements with distinct spacing. *Proc Natl Acad Sci USA* 84(7):1814–1818.
24. Via A, Ferrè F, Brannetti B, Valencia A, Helmer-Citterich M (2000) Three-dimensional view of the surface motif associated with the P-loop structure: *cis* and *trans* cases of convergent evolution. *J Mol Biol* 303(4):455–465.
25. Schmidt G, et al. (1996) Biochemical and biological consequences of changing the specificity of p21ras from guanosine to xanthosine nucleotides. *Oncogene* 12(1):87–96.
26. Walter M, Clark SG, Levinson AD (1986) The oncogenic activation of human p21ras by a novel mechanism. *Science* 233(4764):649–652.
27. Nordmann M, et al. (2010) The Mon1-Ccz1 complex is the GEF of the late endosomal Rab7 homolog Ypt7. *Curr Biol* 20(18):1654–1659.
28. Kucharczyk R, Kierzek AM, Slonimski PP, Rytka J (2001) The Ccz1 protein interacts with Ypt7 GTPase during fusion of multiple transport intermediates with the vacuole in *S. cerevisiae*. *J Cell Sci* 114(Pt 17):3137–3145.
29. Cabrera M, Ungermann C (2013) Guanine nucleotide exchange factors (GEFs) have a critical but not exclusive role in organelle localization of Rab GTPases. *J Biol Chem* 288(40):28704–28712.
30. Scapin SM, et al. (2006) The crystal structure of the small GTPase Rab11b reveals critical differences relative to the Rab11a isoform. *J Struct Biol* 154(3):260–268.
31. Langemeyer L, et al. (2014) Diversity and plasticity in Rab GTPase nucleotide release mechanism has consequences for Rab activation and inactivation. *eLife* 3:e01623.
32. Gasper R, Thomas C, Ahmadian MR, Wittinghofer A (2008) The role of the conserved switch II glutamate in guanine nucleotide exchange factor-mediated nucleotide exchange of GTP-binding proteins. *J Mol Biol* 379(1):51–63.
33. Gavriljuk K, et al. (2012) Catalytic mechanism of a mammalian Rab·RabGAP complex in atomic detail. *Proc Natl Acad Sci USA* 109(52):21348–21353.
34. Mihai Gazdag E, et al. (2013) Mechanism of Rab1b deactivation by the *Legionella pneumophila* GAP LepB. *EMBO Rep* 14(2):199–205.
35. Pan X, Eathiraj S, Munson M, Lambright DG (2006) TBC-domain GAPs for Rab GTPases accelerate GTP hydrolysis by a dual-finger mechanism. *Nature* 442(7100):303–306.
36. Ostermeier C, Brunger AT (1999) Structural basis of Rab effector specificity: Crystal structure of the small G protein Rab3A complexed with the effector domain of rabphilin-3A. *Cell* 96(3):363–374.
37. Pereira-Leal JB, Seabra MC (2000) The mammalian Rab family of small GTPases: Definition of family and subfamily sequence motifs suggests a mechanism for functional specificity in the Ras superfamily. *J Mol Biol* 301(4):1077–1087.
38. Pylypenko O, et al. (2006) Structure of doubly prenylated Ypt1:GDI complex and the mechanism of GDI-mediated Rab recycling. *EMBO J* 25(1):13–23.
39. Taussig D, Lipatova Z, Kim JJ, Zhang X, Segev N (2013) Trs20 is required for TRAPP II assembly. *Traffic* 14(6):678–690.
40. Kim YG, et al. (2006) The architecture of the multisubunit TRAPP I complex suggests a model for vesicle tethering. *Cell* 127(4):817–830.
41. Tokarev AA, et al. (2009) TRAPP II complex assembly requires Trs33 or Trs65. *Traffic* 10(12):1831–1844.
42. Zhang CJ, et al. (2002) Genetic interactions link ARF1, YPT31/32 and TRS130. *Yeast* 19(12):1075–1086.
43. Yamamoto K, Jigami Y (2002) Mutation of TRS130, which encodes a component of the TRAPP II complex, activates transcription of OCH1 in Saccharomyces cerevisiae. *Curr Genet* 42(2):85–93.
44. Sciorra VA, et al. (2005) Synthetic genetic array analysis of the PtdIns 4-kinase Pik1p identifies components in a Golgi-specific Ypt31/rab-GTPase signaling pathway. *Mol Biol Cell* 16(2):776–793.
45. Levine TP, et al. (2013) Discovery of new Longin and Roadblock domains that form platforms for small GTPases in Ragulator and TRAPP-II. *Small GTPases* 4(2):62–69.
46. Choi C, et al. (2011) Organization and assembly of the TRAPPII complex. *Traffic* 12(6):715–725.
47. McDonald CM, Fromme JC (2014) Four GTPases differentially regulate the Sec7 Arf-GEF to direct traffic at the trans-Golgi network. *Dev Cell* 30(6):759–767.
48. Todd RB, Davis MA, Hynes MJ (2007) Genetic manipulation of *Aspergillus nidulans*: Meiotic progeny for genetic analysis and strain construction. *Nat Protoc* 2(4):811–821.
49. Arst HN, Jr, Hernández-Gonzalez M, Peñalva MA, Pantazopoulou A (2014) GBF/Gea mutant with a single substitution sustains fungal growth in the absence of BIG/Sec7. *FEBS Lett* 588(24):4799–4806.
50. Osmani AH, Oakley BR, Osmani SA (2006) Identification and analysis of essential *Aspergillus nidulans* genes using the heterokaryon rescue technique. *Nat Protoc* 1(5):2517–2526.
51. Abenza JF, et al. (2010) *Aspergillus* RabB[Rab5] integrates acquisition of degradative identity with the long distance movement of early endosomes. *Mol Biol Cell* 21(15):2756–2769.
52. Lenzen C, Cool RH, Wittinghofer A (1995) Analysis of intrinsic and CDC25-stimulated guanine nucleotide exchange of p21ras-nucleotide complexes by fluorescence measurements. *Methods Enzymol* 255:95–109.
53. Liu HL, et al. (2010) Single-step affinity purification for fungal proteomics. *Eukaryot Cell* 9(5):831–833.

CELL BIOLOGY